Comparing different profiles to characterize the atmosphere for three MODIS TIR bands

Lluís Pérez-Planells, Vicente García-Santos and Vicente Caselles

Department of Earth Physics and Thermodynamics, Faculty of Physics, University of Valencia, 46100 Valencia, Spain.

Corresponding author e-mail: Vicente.Caselles@uv.es

ABSTRACT

Accurate Land surface temperature (LST) retrievals from sensors aboard orbiting satellites are dependent on the corresponding atmospheric correction, especially in the Thermal InfraRed (TIR) spectral domain (8-14 μm). To remove the atmospheric effects from at-sensor measured radiance in the TIR range it is needed to characterize the atmosphere by means of three specific variables; the upwelling path and the hemispherical downwelling radiances plus the atmospheric transmissivity. Those variables can be derived from the previous knowledge of vertical atmospheric profiles of air temperature and relative humidity at different geo-potential heights and pressures.

In this work, the above mentioned atmospheric variables were analyzed for three specific weather station site located in Spain, at three different altitudes. These variables were calculated with atmospheric profiles retrieved from three different sources; The National Centers for Environmental Prediction (NCEP) web-tool atmospheric profiles calculator, the MODIS (MOD07) product and the radiosoundings available on the web of the University of Wyoming (WYO), which are launched by the Agencia Estatal de Meteorologia (AEMET), in the particular case of Spain. Atmospheric profiles from 2010 to 2013 were obtained to carry out the present study.

Results from comparison of these three different atmospheric profiles show that the NCEP profiles characterize the atmosphere in a better manner than MOD07. Average results values of the three MODIS spectral bands 29, 31 and 32 show a BIAS of 0.06 $Wm^{-2}\mu m^{-1}sr^{-1}$ and RMSE of ±0.2 $Wm^{-2}\mu m^{-1}sr^{-1}$ for upwelling radiance, a BIAS of 0.13 $Wm^{-2}\mu m^{-1}sr^{-1}$ and RMSE of ±0.3 $Wm^{-2}\mu m^{-1}sr^{-1}$ for the donwelling radiance and a BIAS of -0.008 and RMSE of ±0.03 for the atmospheric transmissivity.

In terms of simulated LST, these errors yield a deviation of ±0.9 K when applying a single-channel method.

Keywords: NCEP; MOD07; Radiosoundings; LST; Atmospheric profiles; MODTRAN.

1. INTRODUCTION

Surface radiance measurements taken by Remote Sensing instruments aboard satellites are affected by the atmosphere. In the particular case of the thermal infrared region (3-14 μm), there exists two specific spectral ranges located at 3.7-4.1 μm and 8-14 μm, where the atmosphere shows the lowest radiative effect, mainly due to the water vapor content (W).

The Land Surface Temperature (LST) is a variable of great interest in numerous meteorological and climatological studies, and its accurate retrieval is of prime interest to estimate energy and water fluxes budgets between the surface and atmosphere (Sánchez et al., 2011 and 2014). The main concerns in retrieving LST from satellite data are the atmospheric and emissivity correction (Jiang and Liu, 2014). Currently LST can be obtained from several algorithms dependent on the sensor specifications (Zhou et al., 2012). Two of these techniques are the single-channel (SC, Vlassova et al., 2014) and the Temperature and Emissivity Separation (TES, Hulley et al., 2014) methods. Both algorithms derive the LST from inversion of the radiative transfer equation (RTE), which at the same time needs the previous knowledge of a characterized atmosphere, among other factors. The radiation measured with

a radiometric sensor is composed of a double contribution: first, the radiation directly emitted by the surface, and secondly, the radiation reflected in the surface, coming from the surroundings and the atmosphere. In addition, if the measurement is taken from satellite, the atmosphere contributes in two different ways: on the one hand, absorbing part of the surface radiation and in the other, emitting radiation directly to the sensor. RTE connects the at-sensor radiation and the radiation emitted by the surface through an energy balance defined as:

$$L_i^{TOA} = \tau_i\left[\varepsilon_i B_i(T) + (1-\varepsilon_i)L_{i,hem}^{\downarrow}\right] + L_i^{\uparrow}(\theta) \quad (1)$$

where τ_i is the atmospheric transmissivity at the spectral range *i*, ε_i is the surface spectral emissivity, $B_i(T)$ is the Planck function for black body spectral radiance at temperature T, $L_{i,hem}^{\downarrow}$ is the downwelling hemispheric radiance, $L_i^{\uparrow}(\theta)$ is the upwelling path radiance at zenith angle θ, and L_i^{TOA} is the radiance measured by the sensor at the top of the atmosphere. All the surface and atmospheric factors exposed in Eq. (1) can be found explicitly defined in the reviewing publication of García-Santos et al. (2010). The W present in the atmosphere affects directly to the value of these atmospheric parameters (τ_i, $L_{i,hem}^{\downarrow}$, $L_i^{\uparrow}(\theta)$).

Nowadays, the most suitable way to characterize the atmosphere is by using a radiative transfer code (RTC, Berk et al., 2011), which calculates the atmospheric factors from introducing vertical profiles of pressure, air temperature and humidity at different levels of altitude. Probably, the best representative profile of the corresponding atmosphere is obtained from radiosounding data, acquired with a launched balloon. However, this data is rarely available at the time and location of the measurements acquisition. As an alternative, there exists the possibility to obtain an atmospheric profile derived from the spectral features of overpassing satellite sensor as well as with interpolating models (in space and time) based on radiosounding data acquired close to a selected point (Jimenez-Muñoz et al., 2010).

The objective of this paper is to analyze differences on the atmospheric variables, τ_i, $L_{i,hem}^{\downarrow}$, $L_i^{\uparrow}(\theta)$, after applying on MODTRAN RTC (Berk et al., 2011) different vertical profiles of

74 cloudless days. These profiles are obtained from three different sources: a) Modeled MODIS
75 spectral measured radiances (MOD07, Borbas et al., 2011) profiles. b) Spatial and temporal
76 interpolated National Centers for Environmental Prediction (NCEP) atmospheric profiles (Barsi
77 et al., 2005). c) Radiosounding data measured by balloons launched by AEMET and showed on
78 the web of the Department of Atmospheric Science in the University of Wyoming (WYO).

79 In previous studies carried out by Coll et al. (2012) and Li et al. (2013), the LST obtained
80 from satellite data using SC methods were compared with in situ ground LST measurements,
81 after applying different atmospheric profiles obtained from the NCEP and the MOD07 product.
82 In both cases, these studies obtained good results for the LST comparison, but MOD07
83 introduced greater errors in the LST retrievals (±1.0 K for NCEP and MOD07 in Coll et al. 2012
84 and ±1.1 K for NCEP and ±1.2 K for MOD07 in Li et al. 2013). This paper faces the same
85 objective pursued by Coll et al. (2012) and Li et al., (2013) but in a different and profuse
86 manner. The most important contribution in this paper is that the comparison of atmospheric
87 parameters obtained from NCEP and MOD07 profiles with in situ radiosounding data has been
88 done for a period of 4 years (from 2010 to 2013), and for three different sites with differences
89 in the heights above sea level as well as in the distances from the corners used by NCEP to
90 interpolate the profiles, yielding to more representative statistical results. In addition, results
91 and statistics from MODIS band 29 (8.4 – 8.7 μm) are included. This band, which is not
92 analyzed before in the other papers, is added to the study. It is important an accurate
93 atmospheric correction between 8.4-8.7 μm, which is required in mineralogical and geological
94 research purposes. For instance, mapping geological presence of minerals, like quartz, based
95 on measurements in the reststrahlen region 8-9 μm, where the emissivity of quartz decreases
96 in a very pronounced manner.

97 Section 2 describes the methodology applied to reach the fixed objective. Section 3,
98 shows the results obtained and the corresponding discussions. A simulation study was carried
99 out in section 4 to evaluate the effect in terms of LST when applying SC method with NCEP

and MOD07 profiles if in-situ radiosounding data is not available. Finally, the main conclusions of the study are given in section 5.

2. MATERIALS AND METHODS

2.1 Site

The three selected sites for the study are located at Spain (Murcia, Zaragoza and Madrid). They have been chosen because, from the different Wyoming radiosounding data available, they represent different altitudes above sea level.

The site situated at lesser height above the sea level is Murcia (62 meters). The radiosoundings are launched at the Territorial Center of AEMET of Murcia, located at 3.5 Km from the city (38^{o} N, 1^{o}9' W).

Another region analyzed is focused on the airport of Zaragoza (41^{o}39' N, 1^{o}1' W) at 264 meters of altitude above sea level, and 10 km west from the city.

Finally, as in the case of Zaragoza, in the Madrid area the radiosoundings are launched at the Airport Adolfo Suarez – Barajas (40^{o}30' N, 3^{o}34' W), located at 611 meters above sea level and 12 Km from the city, in north-east direction.

2.2 Atmospheric Profiles

The spatial and temporal representativeness of radiosounding data is a questionable point in some studies. It is used to consider radiosounding data with a spatial representativeness of 250 km (Huntrieser et al., 1996) and temporal representativeness of 12 hours. But these values could be lower in some cases due to the variability of the atmosphere, as happens in mountain areas as Ebro valley (Merino et al., 2013). Different atmospheric profiles are proposed to analyze in these study.

2.2.1 NCEP

123 The on-line atmospheric correction tool (http://atmcorr.gsfc.nasa.gov, last access
124 February 2015) provides the atmospheric parameters needed to make the atmospheric
125 correction in the thermal band of the satellites Landsat-5, Landsat-7 and Landsat-8. The NCEP
126 provides 1^{o} x 1^{o} representative spatial resolution atmospheric profiles every 6 h, as result of
127 four dimensional meteorological data assimilation, including radiosonde (different from WYO
128 soundings), ground and satellite sounder measurements (Barsi et al, 2005). These profiles are
129 processed at 28 different pressure, air temperature and relative humidity, independently of
130 the surface elevation. The corresponding NCEP outputs of temperature (^{o}C) and relative
131 humidity (%), have assigned errors of ±2 K and ±10%, respectively.

132 *2.2.2 WYO radiosounding data*

133 The Atmospheric Science Department of the University of Wyoming (Laramie, WY,
134 USA) has a database of soundings launched every day at 00:00 and 12:00 UTC at different
135 stations distributed around the world (http://weather.uwyo.edu/upperair/sounding.html, last
136 access February 2015).

137 From this database, vertical profiles of height (km), pressure (hPa), temperature (^{o}C),
138 relative humidity (%) and mixing ratio (g/kg), provided at 64 levels, were downloaded for the
139 selected site between 2010 and 2013.

140 These measured variables have uncertainties of ±1 K for the air temperature and ±10
141 % for relative humidity.

142 *2.2.3 MODIS*

143 MODIS (Moderate Resolutions Imaging Spectroradiometer), aboard Terra platform,
144 operates in 36 spectral bands between 0.645 and 14.235 μm, at 705 km of the Earth's surface.
145 Because the characteristics of its spectral bands, MODIS can be used to generate profiles of
146 temperature, relative humidity and dew point at 20 levels of pre-established pressures.
147 Estimations of W are also provided in the atmospheric product named MOD07 (Borbas et al.,

2011). Attributed errors to atmospheric parameters provided by MOD07 product are: ±1.9 ^{o}C to the temperature, ±4 ^{o}C to the dew point, ±10 % to relative Humidity (Borbas et al., 2011).

2.3 Filtering and processing of atmospheric profiles

For a period from 2010 to 2013, a total of 86 scenes for Murcia, 94 for Zaragoza and 164 for Madrid have been introduced in the MODTRAN5.2.1 (Berk et al., 2011) RTC to carry out the study. To pick the selected scenes, some restrictions have been taken into account.

First we consider as a valid time those days where the satellite passed within 30 minutes of the balloon launching. After this first filtering, free of clouds MOD07 scenes over our study region were selected by using the byte codification offered by the MOD07 product, which qualify each pixel as cloudless or not. In a range of 5x5 pixels (Borbas et al., 2011), we require a minimum of 20 cloudless pixels.

Finally, only those days for which the three different profiles were available were selected for this study, obtaining the results that are compared in the next section.

The atmospheric parameters obtained from running MODTRAN5 are presented in the corresponding spectral range to the MODIS bands 29 (8.55 μm), 31 (11 μm) and 32 (12 μm).

3. RESULTS & DISCUSSIONS

3.1 Sensitivity analysis

The uncertainty for each of the retrieved parameters is calculated from the uncertainties associated to the different parameters of the profiles commented in section 2.2. The process to calculate the uncertainty associated to the different parameters that characterize the atmosphere is explained. First, MODTRAN is run with the original profiles, then, MODTRAN is run again with profiles that include the original profiles plus the uncertainty associated to their parameters. Finally, the uncertainty associated to each parameter τ_i,

$L_{i,hem}^{\downarrow}$, $L_i^{\uparrow}(\theta)$ and W is obtained calculating the difference of the parameters retrieved from the original profiles and the parameters retrieved from the profiles with the associated error.

Table 1 shows some statistics rescued from the uncertainties calculated for the atmospheric parameters τ_i, $L_{i,hem}^{\downarrow}$, $L_i^{\uparrow}(\theta)$ of the three sources. These values are calculated taking all data available per band and parameter, not dividing the data for each site.

Insert Table 1 here

The average uncertainty associated to each parameter is lesser for the parameters obtained from MOD07 product, with average values lesser than ±0.5 $Wm^{-2}\mu m^{-1}sr^{-1}$ for $L_i^{\uparrow}(\theta)$, ±0.6 $Wm^{-2}\mu m^{-1}sr^{-1}$ for $L_{i,hem}^{\downarrow}$ and ±0.07 for τ_i. For these cases, the 75% of the uncertainties are under values of ±0.7 $Wm^{-2}\mu m^{-1}sr^{-1}$ for $L_i^{\uparrow}(\theta)$, ±0.8 $Wm^{-2}\mu m^{-1}sr^{-1}$ for $L_{i,hem}^{\downarrow}$ and ±0.09 for τ_i. In the case of NCEP parameters, the uncertainties are higher, with average values lesser than ±0.8 $Wm^{-2}\mu m^{-1}sr^{-1}$, ±1.1 $Wm^{-2}\mu m^{-1}sr^{-1}$ and ±0.11 for $L_i^{\uparrow}(\theta)$, $L_{i,hem}^{\downarrow}$ and τ_i, respectively. For these cases, the 75% of the uncertainties are minor than ±1.13 $Wm^{-2}\mu m^{-1}sr^{-1}$, ±1.5 $Wm^{-2}\mu m^{-1}sr^{-1}$ and ±0.14 for $L_i^{\uparrow}(\theta)$, $L_{i,hem}^{\downarrow}$ and τ_i, respectively. And for WYO parameters, average uncertainties are lesser than ±0.6 $Wm^{-2}\mu m^{-1}sr^{-1}$, ±0.8 $Wm^{-2}\mu m^{-1}sr^{-1}$ and ±0.08 for $L_i^{\uparrow}(\theta)$, $L_{i,hem}^{\downarrow}$ and τ_i, respectively. For these cases, the 75% of the uncertainties are down to ±0.8 $Wm^{-2}\mu m^{-1}sr^{-1}$, ±1.1 $Wm^{-2}\mu m^{-1}sr^{-1}$ and ±0.11 for $L_i^{\uparrow}(\theta)$, $L_{i,hem}^{\downarrow}$ and τ_i, respectively.

All this uncertainties values correspond to band 32 of each parameter and source, since it is the band with greater associated uncertainties. Moreover, the average values are in most cases equal or very close to the median (Q_2).

The results of uncertainties obtained for W are shown in table 2.

Insert Table 2 here

As happens with the other parameters, W retrieved from NCEP profiles provide the greater uncertainties, with an average of ±0.7 cm, while for MOD07 and WYO they are of 0.23 cm and 0.55 cm. In these cases, the 75% of the parameters have an associated uncertainty lower than ±0.9 cm, ±0.3 cm and 0.7 cm for NCEP, MOD07 and WYO, respectively.

3.2 Total column water vapor content

The quantity of water vapor at the atmosphere in a column per unit area (W) is a factor not used directly in the RTE, but with a key importance in the transmissivity, the upwelling and downwelling radiances retrievals. For instance, in García-Santos et al. (2012) the W is obtained through a relationship of downwelling atmospheric radiances, measured at the TIR region in two different angles (0° and 55°).

Therefore, when no radiosounding data are available from a launched balloon, it is important to assure that the selected alternative atmospheric profile is able to characterize the atmosphere by means of a realistic W.

Insert Figure 1 here

Insert Table 3 here

Figure 1 shows the comparison of the W values from NCEP and MOD07 profiles with those from WYO soundings for the full dataset of each site. Comparing results of figure 1 and table 3, it can be observed that W_{NCEP} fit better with W_{WYO} than W_{MOD07} values for the three areas, with an average correlation of 0.93, a BIAS of 0.02 cm and a RMSE of ± 0.2 cm for Zaragoza and a BIAS of 0.2 cm and a RMSE of ± 0.3 cm for Murcia and Madrid, while W_{MOD07} and W_{WYO} present an average correlation of 0.76, a BIAS of -0.05 cm and a RMSE of ± 0.4 cm for Zaragoza, a BIAS of +0.09 and a RMSE of ± 0.3 cm for Murcia and a BIAS of -0.11 and a RMSE of ± 0.3 cm for Madrid. Note that atmospheric MOD07 profiles show a significant underestimation in the W retrievals respect to W_{WYO} values for wet atmospheres ($W_{WYO} \geq 2.5$

217 cm) on the sites of Zaragoza and Madrid while NCEP profiles retrieve well-correlated W values
218 even for very humid atmospheres ($W_{WYO} \geq 3$ cm), although for Murcia they are overestimated.

219 **3.3 Atmospheric transmissivity**

220 The atmospheric transmissivity (τ) retrieved from the NCEP and MOD07 profiles are
221 also compared with the corresponding values, calculated from radiosounding of the University
222 of Wyoming (τ_{WYO}). Figure 2 shows this comparison between the three selected profiles for the
223 three MODIS thermal bands 29 (8.55 μm), 31 (11 μm) and 32 (12 μm).

224 ***Insert Figure 2 here***

225 ***Insert Table 4 here***

226 Results of τ comparison depicted in Figure 2 and statistics in table 4, show clearly again
227 a better agreement between NCEP profiles and WYO data than MOD07 profiles. Average
228 regression coefficients for NCEP are 0.93 for band 29, and 0.91 for bands 31 and 32. For
229 Murcia and Madrid, τ is underestimated, with BIAS among -0.013 and -0.019, depending on
230 the MODIS band analyzed, while for Zaragoza it is overestimated, with BIAS among 0.006 and
231 0.007. RMSE values are among ±0.02 and ±0.04. Corresponding statistics for MOD07 are:
232 average regression coefficient of 0.71, 0.69 and 0.70 for bands 29, 31 and 32, respectively. In
233 the case of Murcia, τ retrieved is underestimated, with BIAS among -0.07 and -0.05, while for
234 Zaragoza and Madrid it is overestimated, with BIAS values among 0.001 and 0.06. RMSE values
235 for MOD07 are among 0.03 and 0.08. Note that for MOD07 values of BIAS and RMSE values are
236 close to zero as the altitude of the meteorological station is higher. However, for NCEP they
237 are similar for the three areas.

238 NCEP reproduces transmissivity values closer to those obtained from radiosounding
239 data. This is probably due to the good agreement observed between the water vapor retrieved
240 with NCEP and that calculated from WYO soundings data, since W is indirectly included in the

241 transmissivity exponential expression, through W concentration factor (ρ) and the water
242 spectral absorption coefficient (k, see Eq. (4) in García-Santos et al., 2010).

243 **3.4 Upwelling path radiance**

244 The upwelling radiance ($L_{\lambda}^{\uparrow}(\theta)$ or Lup), retrieved from NCEP and MOD07 atmospheric
245 profiles, is compared with that from the radiosoundings of University of Wyoming (Lup_{WYO}).
246 The results are shown in figure 3 for the three thermal bands of sensor MODIS.

247 ***Insert Figure 3 here***

248 ***Insert Table 5 here***

249 Graphics of figure 3 show a better agreement for NCEP results than for MOD07, when
250 comparing with Lup calculated from WYO profiles. From statistics in table 5, the average
251 regression coefficient for NCEP is 0.95 for band 29 and 0.92 for bands 31 and 32. For Murcia
252 and Madrid, BIAS values are among 0.08 $Wm^{-2}\mu m^{-1}sr^{-1}$ and 0.15 $Wm^{-2}\mu m^{-1}sr^{-1}$, and RMSE
253 among ±0.13 $Wm^{-2}\mu m^{-1}sr^{-1}$ and ±0.3 $Wm^{-2}\mu m^{-1}sr^{-1}$. For Zaragoza, BIAS is of -0.06 $Wm^{-2}\mu m^{-1}sr^{-1}$
254 and -0.07 $Wm^{-2}\mu m^{-1}sr^{-1}$, depending of the spectral band, and RMSE among ±0.16 $Wm^{-2}\mu m^{-1}sr^{-1}$
255 and ±0.3 $Wm^{-2}\mu m^{-1}sr^{-1}$. Considering MOD07, the average regression coefficients for each band
256 are: 0.78, 0.73 and 0.73 for bands 29, 31 and 32, respectively. For Murcia, BIAS is among 0.27
257 $Wm^{-2}\mu m^{-1}sr^{-1}$ and 0.35 $Wm^{-2}\mu m^{-1}sr^{-1}$, and RMSE among ±0.4 $Wm^{-2}\mu m^{-1}sr^{-1}$ and ±0.6 $Wm^{-2}\mu m^{-1}sr^{-1}$.
258 In the cases of Zaragoza and Madrid, BIAS is among -0.16 $Wm^{-2}\mu m^{-1}sr^{-1}$ and -0.49 $Wm^{-2}\mu m^{-1}sr^{-1}$,
259 and RMSE among ±0.3 $Wm^{-2}\mu m^{-1}sr^{-1}$ and ±0.6 $Wm^{-2}\mu m^{-1}sr^{-1}$.

260 In this case, NCEP data seems to fit better to the curve 1:1. This might be linked to the
261 better agreement in terms of transmissivity shown above. Moreover, it is noticed that the BIAS
262 and RMSE values obtained from both sources are better for high altitudes.

3.5 Downwelling hemispheric radiance

The results of the downwelling hemispherical radiances ($L^{\downarrow}_{\lambda,\mathrm{hem}}$ or Ldown) retrieved from the NCEP and product MOD07 profiles, are compared with the radiosoundings of the - University of Wyoming (WYO), and they are depicted on figure 4.

Insert Figure 4 here

Insert Table 6 here

Results from graphics of figure 4 show a better fitting of NCEP than for MODIS compared with WYO data. From information in table 6, the average regression coefficient for NCEP in each band are 0.95 for band 29 and 0.95 for bands 31 and 32. In the case of NCEP, the BIAS obtained for each site ranges among 0.21 $Wm^{-2}\mu m^{-1}sr^{-1}$ and 0.23 $Wm^{-2}\mu m^{-1}sr^{-1}$ for Murcia, -0.014 $Wm^{-2}\mu m^{-1}sr^{-1}$ and 0.07 $Wm^{-2}\mu m^{-1}sr^{-1}$ for Zaragoza and 0.19 $Wm^{-2}\mu m^{-1}sr^{-1}$ and 0.23 $Wm^{-2}\mu m^{-1}sr^{-1}$ for Madrid. RMSE values for the three sites ranges among ±0.2 $Wm^{-2}\mu m^{-1}sr^{-1}$ and ±0.4 $Wm^{-2}\mu m^{-1}sr^{-1}$. Respect to MOD07, average regression coefficients are 0.82, 0.76 and 0.76for bands 29, 31 and 32, respectively. For Murcia, BIAS is among -0.26 $Wm^{-2}\mu m^{-1}sr^{-1}$ and -0.33 $Wm^{-2}\mu m^{-1}sr^{-1}$, -0.41 $Wm^{-2}\mu m^{-1}sr^{-1}$ and -0.65 $Wm^{-2}\mu m^{-1}sr^{-1}$ for Zaragoza and -0.51 $Wm^{-2}\mu m^{-1}sr^{-1}$ and -0.73 $Wm^{-2}\mu m^{-1}sr^{-1}$ for Madrid. RMSE for the three sites are among ±0.4 $Wm^{-2}\mu m^{-1}sr^{-1}$ and ±0.7 $Wm^{-2}\mu m^{-1}sr^{-1}$.

Similar to Lup, the Ldwn depends on the atmospheric transmissivity, so the undervaluation realized for the W in wet atmosphere is here reflected again, for the cases of Zaragoza and Madrid. This effect is stressed for band 32 since water vapor absorption is higher in this spectral range.

4. Simulation study

In order to analyze the uncertainties in terms of temperature retrieved using the atmospheric parameters calculated in this paper, through different sources, a simulation study was carried out using the SC method (Vlassova et al., 2014). The procedure is as follows:

First, for a defined T (in this study three different temperatures were selected: 273 K, 293 K and 313 K) a $B_i(T)$ is calculated and a L_i^{TOA} retrieved trough Eq. (1) at the three MODIS bands 29, 31 and 32. Atmospheric parameters from the WYO profiles are used to obtain L_i^{TOA} and the surface emissivity (ε_i) used in this case, is the corresponding to a rice crop, which has well characterized value of 0.983 ± 0.005 (Coll et al., 2014). Moreover, this value is almost constant in the thermal region.

In a second step, a new $B_i(T)$ is calculated through Eq. (1), using the corresponding atmospheric variables obtained from NCEP or MOD07 profiles and the previous calculated L_i^{TOA}. This new $B_i(T)$ is inverted and a new T retrieved. Table 7 shows the average BIAS between original T and those temperatures (for the three selected temperatures) obtained from NCEP and MOD07 profiles and RMSE calculated from all the cases analyzed, at the three MODIS thermal bands.

Insert Table 7 here

Average results for these three temperatures show that the lowest error are obtained for bands 29 (8.55 µm) and 31 (11 µm). Taking average results of the three sites per MODIS band, band 29 shows a BIAS of +1.3 K and RMSE of ±0.6 K for NCEP and 1.2 K and ±1.9 K for MOD07. For band 31, NCEP shows a BIAS of -0.04 K and RMSE of ±0.6 K and for MOD07 the study shows a BIAS of +0.6 K and RMSE of ±1.5 K. The greatest error is obtained for band 32 (12 µm) where the NCEP profiles show a BIAS of -0.05 K and RMSE of ±0.8 K, and BIAS of 0.7 K and RMSE of ±2 K for MOD07, this is reasonable since this band is the most sensitive to water vapor.

In summary, the well characterization obtained for the atmospheric parameters τ_i, $L_{i,hem}^{\downarrow}$, $L_i^{\uparrow}(\theta)$, especially for bands 29and 31, affects directly to the LST retrieval, obtaining lower uncertainties in these cases. Moreover, for MOD07 band 31 obtains better results for LST since it is the less affected band by the water vapor. It is noticed that RMSE obtained are lower in the cases from Madrid, where the altitude is higher and the atmosphere might be better characterized, particularly in profile got from satellite data. These results are in agreement with Coll et al. (2012) for which band 31 has BIAS of -0.3 K and RMSE of ±0.6K for NCEP and BIAS of -0.5 K and RMSE of ±0.8 K for MOD07, and Li et al. (2013) with BIAS of 0.37 K and RMSE of ±1.16 K for NCEP using the IRS thermal band (10.5 -12.5 μm) and BIAS of 0.20 K and RMSE of ±1.2 K for MOD07, concluding that NCEP offers less error than MOD07 profiles.

5. CONCLUSIONS

This work has analyzed the differences appeared when characterizing the atmosphere from different atmospheric profiles: NCEP, MOD07_L2 product and radiosoundings from the University of Wyoming (used as reference).

Atmospheric parameters in the TIR region 8-14 μm (upwelling radiance, downwelling hemispheric radiance and atmospheric transmissivity) were obtained for three thermal bands (29, 31 and 32) of sensor MODIS.

It is concluded that both NCEP and MOD07 profiles show an acceptable agreement with results from WYO profiles. However, despite NCEP profiles show greater uncertainties estimating the atmospheric parameter, because their spatial and temporal interpolation procedure, results show a better fit with the reference WYO values at the three spectral bands. Conversely, the values obtained from MOD07 show lower uncertainties than the NCEP, but their results are more scattered and less correlated with WYO results. So water vapour content

is usually underestimated for MOD07, in particular for wet atmospheres (w > 2.5 cm) and high altitudes.This underestimation is propagated to the others parameters, underestimating in the same way upwelling and downwelling radiance and overestimating the atmospheric transmissivity.

A simulation study was carried out to analyze the effect of each atmospheric profile retrieving the surface temperature when applying the SC method. Results showed RMSE between ±0.6-±0.9 K for NCEP and between ±1.3-±3 K for MOD07, depending on the spectral band and the altitude of the study site. So for bands 29 and 31, temperature uncertainties show the best results, probably because band 32 is more affected by the water vapor. Moreover, it is observed better results on the LST retrievals for high altitudes, leading to lower errors in the way that the altitude is greater. This is probably due to MOD07 product get less data for lower altitudes. For example, in the case of Murcia, the first data level is around 120 meters, 60 meters over the ground altitude. While for higher altitudes, that measure is more accurate.

Radiosounding data is probably the best way to characterize the atmosphere, but rarely there are radiosoundings available at the time and location of interest. This study has shown that using as alternative NCEP profiles leads to optimal results when characterizing the atmosphere. In addition, good results are obtained for MODIS band 29 (8.55 μm), which has not been studied previously in other works, with uncertainties similar to those obtained for MODIS band 31 (11 μm).

Acknowledgements

This study was supported by the Spanish Ministry of Economy and Competitiveness, through projects CGL2013-46862-C2-1-P and CGL2011-30433-C02-02. We also want to thank the Government of Generalitat Valenciana for the support this study through the project PROMETEOII/2014/086.

6. References

Barsi, J. A., Schott, J. R., Palluconi, F. D., Hook, S. J., 2005. Validation of a Web-Based Atmospheric Correction Tool for Single Thermal Band Instruments. Earth Observing Systems X, Proc. SPIE Vol. 5882, August 2005, San Diego, CA.

Berk, Anderson, G. P., Acharya, P. K., Shettle, E. P., 2011. MODTRAN®5.2.1 USER'S MANUAL.

Borbas, E. E., Seemann, S. W., Kern, A., Moy, L., Li, J., Gumley, L., Menzel, P., 2011. Modis atmospheric profile retrieval algorithm theoretical basis document, Collection 6, Version 7, University of Wisconsin-Madison.

Coll, C., García-Santos, V., Niclòs, R., Caselles, V., 2014. Validation of the new MODIS land surface and emissivity algorithm (MOD21) with ground measurements at the Valencia test site. Remote Sensing of Environment, (in review).

Coll, C., Caselles, V., Valor, E., Niclòs, R., 2012. Comparison between different sources of atmospheric profiles for land surface temperature retrieval from single channel thermal infrared data. Remote Sensing of Environment, 117, 199-210.

García-Santos, V., Valor, E., Caselles, V., 2010. Determination of the surface temperature by remote sensing. Tethys, 7, 67-75.

García-Santos, V., Galve, J. M., Valor, E., Caselles, V., Coll, C., 2012. Estimation of atmospheric water vapour content from direct measurements of radiance in the thermal infrared region. Remote Sens. Letters., vol. 3, no. 1, pp. 31–38. DOI: 10.1080/01431161.2010.531060

Hulley, G., Veraverbeke, S., Hook, S., 2014. Thermal-based techniques for land cover change detection using a new dynamic MODIS multispectral emissivity product (MOD21). Remote Sensing of Environment, 140, 755-765.

381 Huntrieser, H., Schiesser, H.H., Schmid, W., Waldvogel, A., 1997. Comparison of traditional and
382 newly developed thunderstorm indices for Switzerland. Weather Forecast. 12, 108-125.

383 Jiang, G.-M., Liu,R., 2014. Retrieval of sea and land surface temperature from SVISSR/FY-
384 2C/D/E measurements. IEEE Transactions on Geosciences and Remote Sensing, 52, 10.

385 Jiménez-Muñoz, J.C., Sobrino, J.A., Mattar, C., Franch, B., 2010. Atmospheric correction of
386 optical imagery from MODIS and Reanalysis atmospheric products. Remote Sensing of
387 Environment, 114, 2195-2210.

388 Li, H., Liu, Q., Du, Y., Jiang, J., Wang, H., 2013. Evaluation of the NCEP and MODIS atmospheric
389 products for single channel land surface temperature retrieval with ground measurements:
390 a case study of HJ-1B IRS data. IEEE journal of selected topics in applied earth observations
391 and remote sensing, 6, 3.

392 Merino, A., García-Ortega, E., López, L., Sánchez, J.L., Guerrero-Higueras, A.M., 2013. Synoptic
393 environment, mesoscale configurations and forecast parameters for hailstorms in
394 Southwestern Europe. Atmos. Res. 122, 183-198.

395 Sánchez, J.M., López-Urrea, R., Rubio, E., Caselles, V., 2011. Determining water use of sorghum
396 from two-source energy balance and radiometric temperatures. Hydrology and Earth
397 System Sciences, 15, 3061-3070.

398 Sánchez, J.M., López-Urrea, R., Rubio, E., González-Piqueras, J., Caselles, V., 2014. Assessing
399 crop coefficients of sunflower and canola using two.source energy balance and thermal
400 radiometry. Agricultural water management, 137, 23-29.

401 Vlassova, L., Perez-Cabello, F., Nieto, H., Martín, P., Riaño, D., Riva, J., 2014. Assesment of
402 methods for land surface temperature retrieval from Landsat-5 TM images applicable to
403 multiscale tree-grass ecosystem modeling. Remote Sensing, 6, 4345-4368.

Zhou, J., Li, J., Zhang, L., Hu, D., Zhan, W., 2012. Intercomparison of methods for esmating land surface temperature from a Landsat-5 TM image in an arid region with low water vapour in the atmosphere. International Journal of Remote Sensing, 33, 2582-2602.

Tables

Table 1. Statistics of the uncertainties obtained for the different atmospheric parameters (Lup, Ldown, τ) in each MODIS spectral band and for the three sources. Max and min represents the maximum and minor value obtained, av is the average uncertainty and Q1, Q2, Q3 are the first, second and third quartile, respectively.

	NCEP						MOD07						WYO					
	BAND 29						BAND 29						BAND 29					
	max	min	av.	Q1	Q2	Q3	max	min	av.	Q1	Q2	Q3	max	min	av.	Q1	Q2	Q3
Lup ($Wm^{-2}\mu m^{-1}sr^{-1}$)	1.1	0.13	0.5	0.3	0.5	0.7	0.8	0.08	0.3	0.2	0.5	0.4	0.7	0.07	0.4	0.2	0.3	0.5
Ldown ($Wm^{-2}\mu m^{-1}sr^{-1}$)	1.5	0.2	0.8	0.5	0.8	1.0	1.0	0.11	0.5	0.3	0.8	0.6	1.1	0.12	0.5	0.3	0.5	0.7
τ	0.11	0.02	0.06	0.05	0.06	0.08	0.09	0.01	0.04	0.03	0.06	0.05	0.09	0.01	0.05	0.04	0.05	0.06
	BAND 31						BAND 31						BAND 31					
Lup ($Wm^{-2}\mu m^{-1}sr^{-1}$)	1.7	0.09	0.7	0.4	0.7	1.0	1.3	0.05	0.5	0.2	0.4	0.6	1.2	0.06	0.5	0.3	0.5	0.7
Ldown ($Wm^{-2}\mu m^{-1}sr^{-1}$)	2.0	0.15	1.0	0.6	1.1	1.4	1.4	0.08	0.6	0.3	0.5	0.7	1.6	0.10	0.7	0.4	0.7	1.0
τ	0.17	0.01	0.09	0.05	0.09	0.12	0.14	0.01	0.06	0.03	0.05	0.08	0.13	0.01	0.06	0.04	0.06	0.09
	BAND 32						BAND 32						BAND 32					
Lup ($Wm^{-2}\mu m^{-1}sr^{-1}$)	1.7	0.12	0.8	0.5	0.9	1.1	1.3	0.07	0.5	0.3	0.5	0.7	1.3	0.08	0.6	0.3	0.6	0.8
Ldown ($Wm^{-2}\mu m^{-1}sr^{-1}$)	2.1	0.2	1.13	0.8	1.2	1.5	1.4	0.10	0.6	0.4	0.6	0.8	1.6	0.13	0.8	0.5	0.8	1.1
τ	0.33	0.02	0.11	0.07	0.12	0.14	0.15	0.01	0.07	0.04	0.07	0.09	0.16	0.01	0.08	0.05	0.08	0.11

Table 2. Statistics of the uncertainties obtained for the water vapour content each source. Max and min represents the maximum and minor value obtained, av is the average uncertainty and Q1, Q2, Q3 are the first, second and third quartile, respectively.

	W (cm)					
	max	**min**	**av**	**Q1**	**Q2**	**Q3**
NCEP	1.4	0.19	0.7	0.5	0.7	0.9
MOD07	0.7	0.004	0.2	0.10	0.19	0.3
WYO	1.1	0.13	0.6	0.4	0.5	0.7

Table 3. Linear regression parameters obtained from the comparison of W retrieved between the NCEP-WYO and MOD07-WYO (figure 1). From the fitting, m represents the slope, n is the offset, r^2 is the regression coefficient and σ the standard deviation. In addition, it is shown the average BIAS and RMSE of the depicted points.

NCEP - WYO	**m**	**n**	**r^2**	**σ**	**BIAS**	**RMSE**
Murcia	1.07	0.08	0.93	0.2	0.2	0.3
Zaragoza (cm)	0.93	0.13	0.92	0.2	0.018	0.2
Madrid	0.99	0.22	0.94	0.15	0.2	0.3
MOD07 - WYO	**m**	**n**	**r^2**	**σ**	**BIAS**	**RMSE**
Murcia	0.99	0.11	0.80	0.3	0.09	0.3
Zaragoza (cm)	0.80	0.26	0.74	0.4	-0.05	0.4
Madrid	0.76	0.20	0.74	0.3	-0.11	0.3

Table 4. Linear regression parameters obtained from the comparison of transmissivity retrieved for three MODIS TIR bands between the NCEP-WYO and MOD07-WYO (figure 2), for three different sites. From the fitting, m represents the slope, n is the offset, r^2 is the regression coefficient and σ the standard deviation. In addition, it is show the average BIAS and RMSE of the depicted points.

	NCEP						MOD07					
	MURCIA						MURCIA					
	m	n	r^2	σ	BIAS	RMSE	m	n	r^2	σ	BIAS	RMSE
τ_{29}	1.01	-0.02	0.93	0.02	-0.013	0.02	0.98	-0.05	0.74	0.04	-0.07	0.08
τ_{31}	1.04	-0.05	0.91	0.03	-0.016	0.03	0.99	-0.04	0.74	0.05	-0.05	0.07
τ_{32}	1.04	-0.05	0.91	0.03	-0.019	0.04	0.96	-0.03	0.74	0.06	-0.06	0.08
	ZARAGOZA						ZARAGOZA					
τ_{29}	0.92	0.06	0.92	0.02	0.006	0.02	0.71	0.25	0.76	0.03	0.04	0.05
τ_{31}	0.90	0.09	0.89	0.03	0.007	0.03	0.61	0.37	0.72	0.03	0.05	0.06
τ_{32}	0.91	0.08	0.89	0.04	0.009	0.04	0.63	0.35	0.73	0.04	0.06	0.08
	MADRID						MADRID					
τ_{29}	0.94	0.03	0.95	0.013	-0.015	0.02	0.71	0.22	0.63	0.03	0.0014	0.03
τ_{31}	0.95	0.03	0.93	0.017	-0.013	0.02	0.61	0.35	0.62	0.03	0.02	0.04
τ_{32}	0.94	0.03	0.93	0.02	-0.016	0.03	0.62	0.34	0.63	0.04	0.03	0.05

425 **Table 5. Linear regression parameters obtained from the comparison of upwelling radiance retrieved for three MODIS TIR bands between the NCEP-WYO**

426 **and MOD07-WYO (figure 2), for three different sites. From the fitting, m represents the slope, n is the offset, r^2 is the regression coefficient and σ the**

427 **standard deviation. In addition, it is show the average BIAS and RMSE of the depicted points.**

		NCEP						MOD07					
		MURCIA						MURCIA					
		m	n	r^2	σ	BIAS	RMSE	m	n	r^2	σ	BIAS	RMSE
Lup_{29}	($Wm^{-2}\mu m^{-1}sr^{-1}$)	1.03	0.03	0.95	0.15	0.08	0.17	1.02	0.24	0.85	0.3	0.3	0.4
Lup_{31}		1.05	0.05	0.92	0.2	0.13	0.3	1.01	0.31	0.80	0.4	0.3	0.5
Lup_{32}		1.04	0.07	0.92	0.3	0.15	0.3	0.98	0.39	0.79	0.4	0.4	0.6
		ZARAGOZA						ZARAGOZA					
Lup_{29}	($Wm^{-2}\mu m^{-1}sr^{-1}$)	0.93	0.05	0.94	0.15	-0.06	0.16	0.72	0.13	0.80	0.2	-0.3	0.4
Lup_{31}		0.91	0.06	0.90	0.2	-0.06	0.2	0.61	0.12	0.74	0.3	-0.4	0.5
Lup_{32}		0.91	0.08	0.90	0.3	-0.07	0.3	0.62	0.13	0.75	0.3	-0.5	0.6
		MADRID						MADRID					
Lup_{29}	($Wm^{-2}\mu m^{-1}sr^{-1}$)	1.00	0.11	0.97	0.10	0.11	0.15	0.70	0.26	0.70	0.2	-0.16	0.3
Lup_{31}		0.98	0.13	0.94	0.14	0.11	0.18	0.59	0.22	0.65	0.2	-0.2	0.3
Lup_{32}		0.97	0.17	0.94	0.16	0.13	0.13	0.59	0.24	0.65	0.3	-0.3	0.4

428

429

430

Table 6. Linear regression parameters obtained from the comparison of downwelling hemispheric radiance retrieved for three MODIS TIR bands between the NCEP-WYO and MOD07-WYO (figure 2), for three different sites. From the fitting, m represents the slope, n is the offset, r^2 is the regression coefficient and σ the standard deviation. In addition, it is show the average BIAS and RMSE of the depicted points.

	NCEP						MOD07					
	MURCIA						MURCIA					
	m	n	r^2	σ	BIAS	RMSE	m	n	r^2	σ	BIAS	RMSE
$Ldown_{29}$	1.08	0.00	0.94	0.26	0.2	0.3	0.90	0.02	0.89	0.30	-0.3	0.4
$Ldown_{31}$ ($Wm^{-2}\mu m^{-1}sr^{-1}$)	1.06	0.07	0.92	0.34	0.2	0.4	0.78	0.19	0.83	0.37	-0.3	0.5
$Ldown_{32}$	1.05	0.09	0.92	0.37	0.2	0.4	0.79	0.22	0.83	0.43	-0.3	0.5
	ZARAGOZA						ZARAGOZA					
$Ldown_{29}$	0.98	0.05	0.94	0.23	-0.014	0.2	0.78	0.15	0.81	0.36	-0.4	0.5
$Ldown_{31}$ ($Wm^{-2}\mu m^{-1}sr^{-1}$)	0.93	0.08	0.91	0.32	-0.06	0.3	0.66	0.15	0.75	0.40	-0.6	0.7
$Ldown_{32}$	0.94	0.08	0.91	0.35	-0.07	0.4	0.68	0.16	0.76	0.46	-0.7	0.8
	MADRID						MADRID					
$Ldown_{29}$	1.04	0.14	0.97	0.15	0.2	0.3	0.65	0.26	0.78	0.28	-0.5	0.6
$Ldown_{31}$ ($Wm^{-2}\mu m^{-1}sr^{-1}$)	0.99	0.20	0.95	0.20	0.19	0.3	0.50	0.24	0.70	0.27	-0.6	0.7
$Ldown_{32}$	0.98	0.26	0.95	0.23	0.2	0.3	0.51	0.26	0.70	0.33	-0.7	0.8

436 **Table 7. BIAS and RMSE calculated from the comparison between the original LST and those**
437 **retrieved using NCEP or MOD07 atmospheric parameters for three MODIS bans (29, 31, 32)**
438 **in each one of the selected sites.**

	MURCIA			
	NCEP		MOD07	
Band	**BIAS (K)**	**RMSE (K)**	**BIAS (K)**	**RMSE (K)**
29	0.08	0.6	3	3
31	-0.05	0.6	1.2	1.9
32	-0.05	0.8	1.6	3
	ZARAGOZA			
29	0.15	0.6	0.15	1.3
31	0.011	0.7	-0.03	1.4
32	-0.004	0.9	-0.07	2
	MADRID			
29	0.03	0.6	1.3	1.7
31	-0.09	0.6	0.6	1.2
32	-0.09	0.7	0.8	2

439

FIGURE CAPTIONS

Figure 1. Differences NCEP-WYO, and MOD07-WYO, versus W.

Figure 2. Linear regression of the comparison between NCEP and WYO (three top graphs) and MODIS-WYO (three bottom graphs), in terms of estimated τ for the three MODIS thermal bands 29 (8.55 μm), 31 (11 μm) and 32 (12 μm).

Figure 3. Linear regression of the comparison between NCEP and WYO (three top graphs) and MODIS-WYO (three bottom graphs), in terms of estimated Lup for the three MODIS thermal bands 29 (8.55 μm), 31 (11 μm) and 32 (12 μm).

Figure 4. Linear regression of the comparison between NCEP and WYO (three top graphs) and MODIS-WYO (three bottom graphs), in terms of estimated Ldown for the three MODIS thermal bands 29 (8.55 μm), 31 (11 μm) and 32 (12 μm).

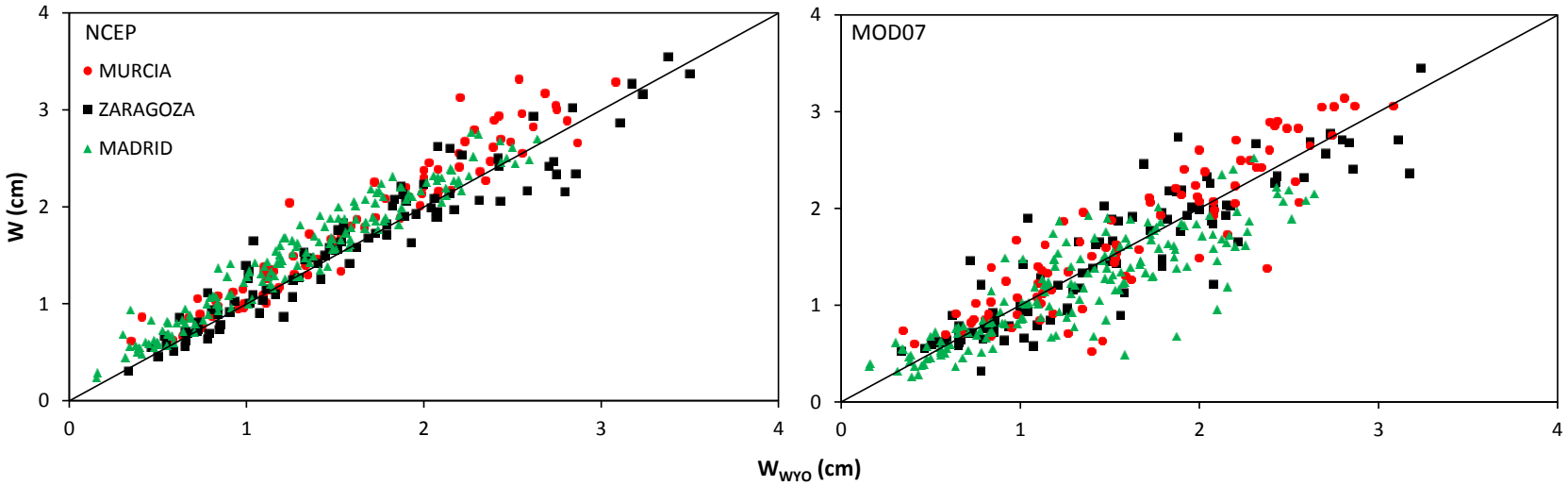

Figure 1

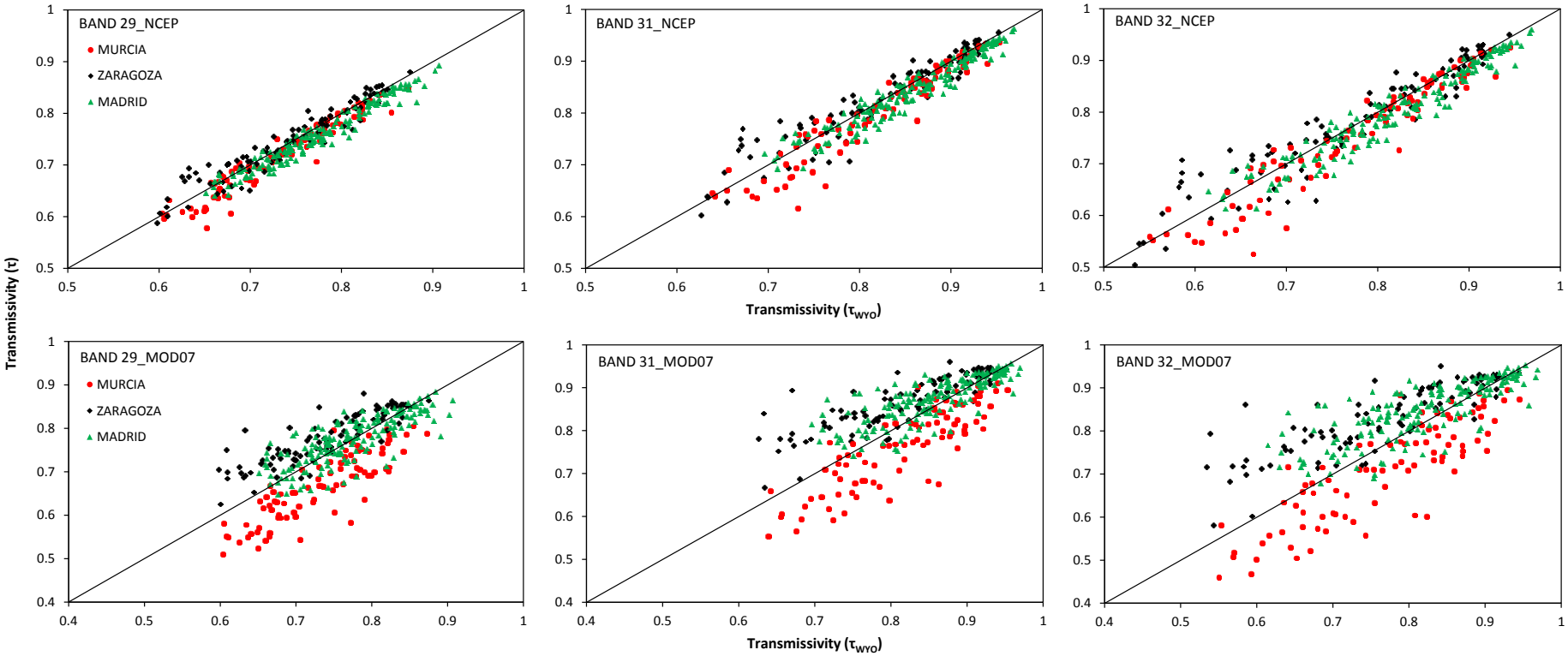
BAND 29_NCEP
MURCIA
ZARAGOZA
MADRID
BAND 31_NCEP
BAND 32_NCEP
BAND 29_MOD07
BAND 31_MOD07
BAND 32_MOD07
Transmissivity (τ)
Transmissivity (τWYO)
Transmissivity (τWYO)

Figure 2

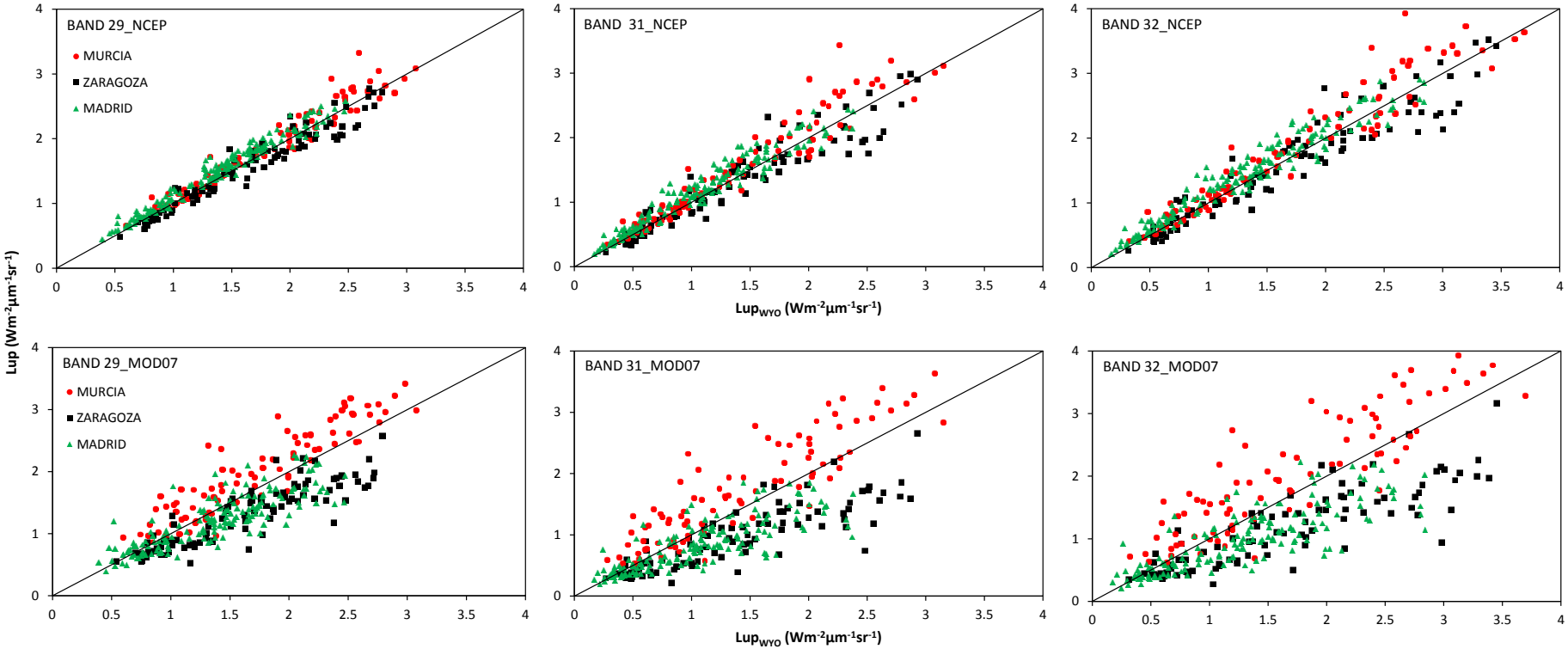
BAND 29_NCEP
MURCIA
ZARAGOZA
MADRID
BAND 31_NCEP
BAND 32_NCEP
BAND 29_MOD07
BAND 31_MOD07
BAND 32_MOD07
Lup (Wm-2µm-1sr-1)
Lup_WYO (Wm-2µm-1sr-1)

Figure 3

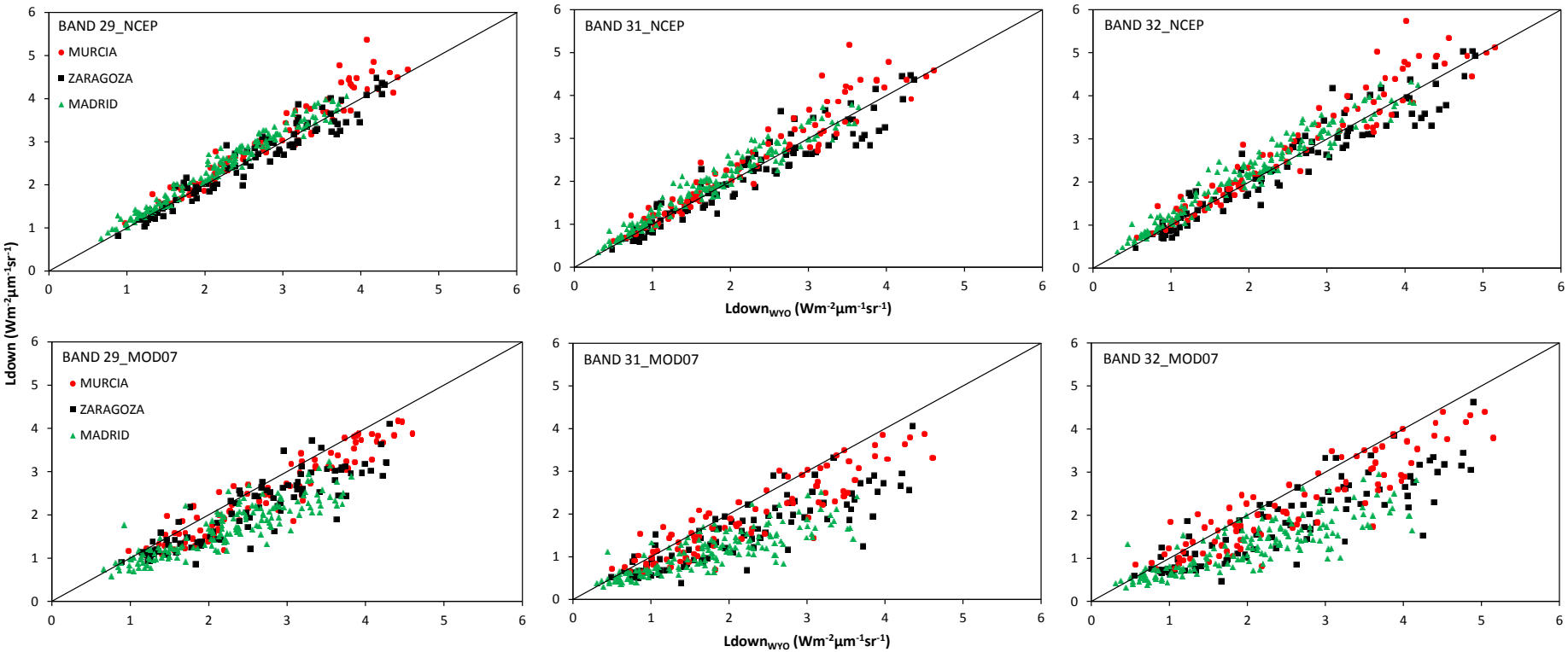
BAND 29_NCEP
MURCIA
ZARAGOZA
MADRID
BAND 31_NCEP
BAND 32_NCEP
BAND 29_MOD07
BAND 31_MOD07
BAND 32_MOD07
Ldown (Wm-2µm-1sr-1)
Ldown_WYO (Wm-2µm-1sr-1)

Figure 4